DAΦNE TECHNICAL NOTE

INFN - LNF, Accelerator Division

Frascati, November 8, 1994

Note: **MM-3**

MAGNETIC MEASUREMENTS ON THE FIRST PERMANENT MAGNET QUADRUPOLES (Q1) OF THE KLOE INTERACTION REGION

B. Bolli, F. Iungo, M. Preger, C. Sanelli, M. Modena,
M. Sardone, F. Sgamma, M. Troiani,

1. INTRODUCTION

The first two quadrupoles of the KLOE low-β interaction region (Q1) have been realized with the permanent magnet technique for the main following reasons:

- since permanent magnets are almost completely transparent to external fields, the solenoidal field of the KLOE detector and the quadrupole field add up linearly;

- with the permanent magnet technique the quadrupole can be realized with very small transverse dimensions, as compared with conventional electromagnets, thus allowing the maximum free solid angle to the experiment.

The two quadrupoles have been built by ASTER Enterprises Inc., Massachussets, following the LNF Specification, recalled in Tab. 1 and Fig. 1.

Table 1 - Permanent magnet quadrupoles Specification

Nominal gradient (T/m)	5.93
Integrated gradient (T)	1.186±0.5%
Good field region (mm)	30
Integrated field quality $\lvert\Delta B/B\rvert$	5×10^{-4}
Maximum mismatch of integrated gradient between two quads	1×10^{-3}
Minimum inside radius (mm)	52
Maximum outside radius (mm)	see Spec. Drawing
Magnetic length (mm)	200±1
REM Stabilization Temperature (°C)	150
REM Type	SM_2CO_{17}
Magnet construction	2-half vertically split

The construction drawing of the magnet is shown in Fig. 2, while Fig. 3 gives the detail of the splitting system.

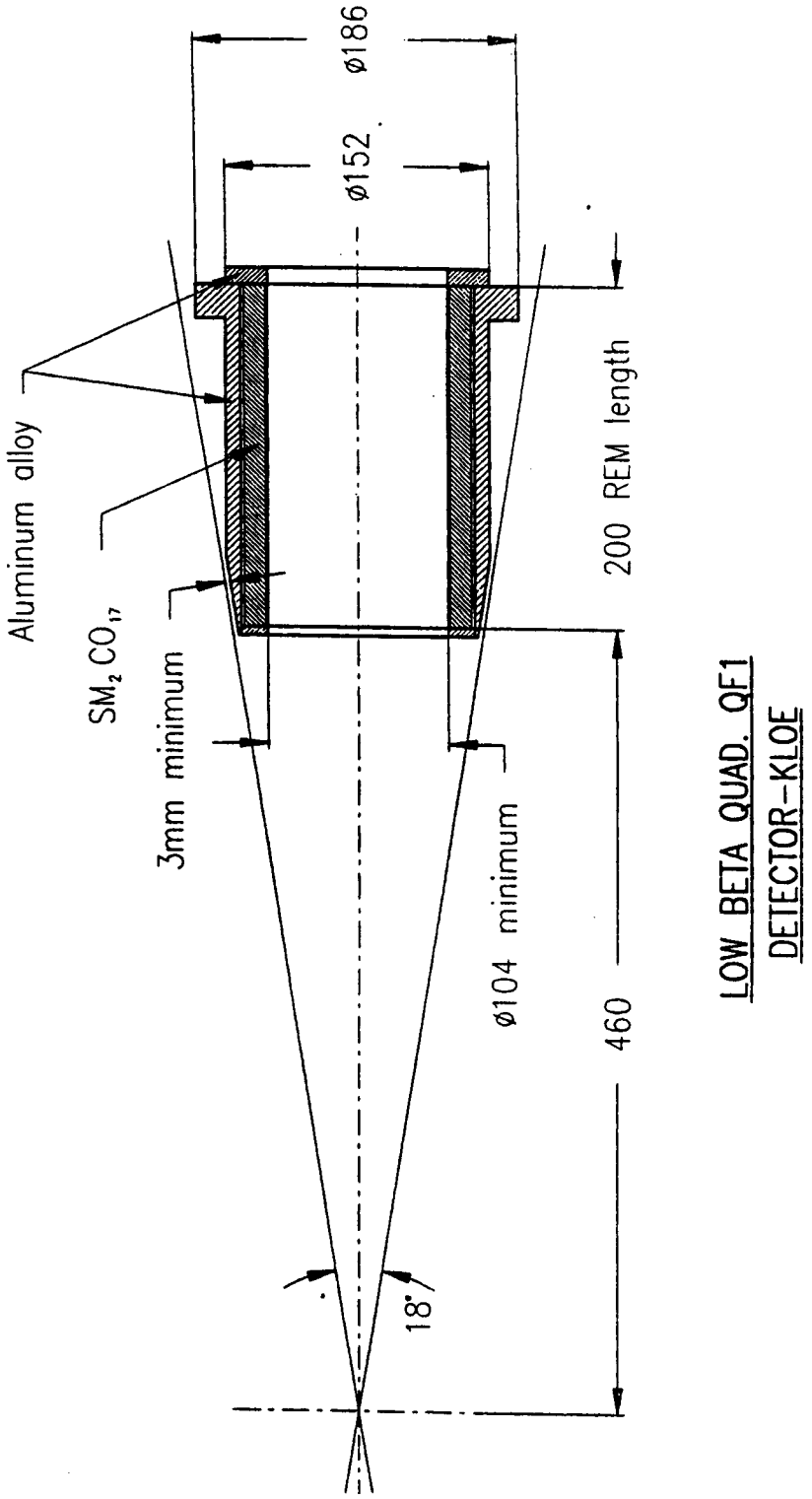

Figure 1 - Specification drawing for first low-β quadrupole in the KLOE Interactcion Region

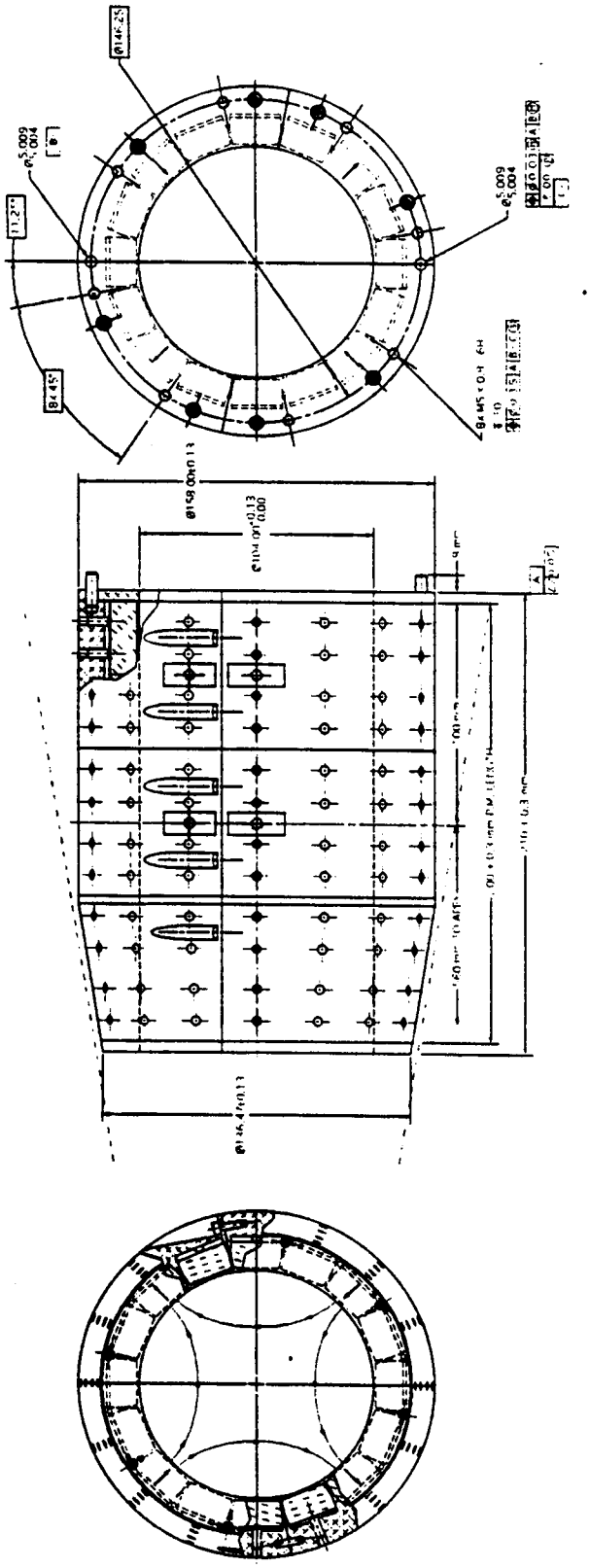

Figure 2 - ASTER quadrupole drawing

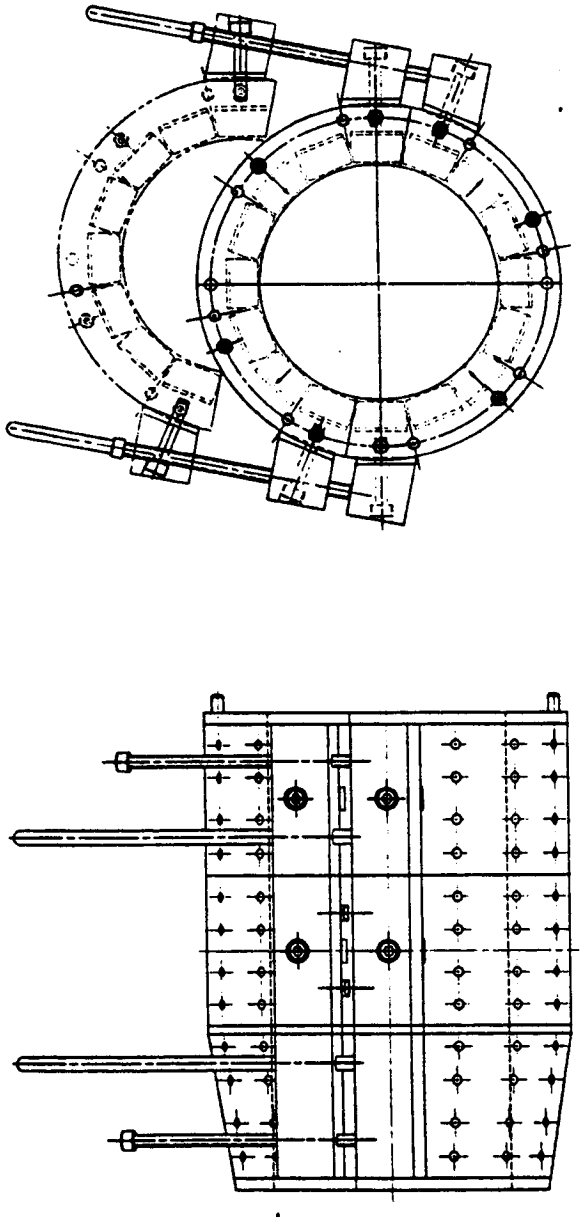

Figure 3 - ASTER quadrupole splitting system

2. MAGNETIC MEASUREMENTS AT ASTER AND LNF

The two quadrupoles have been measured at the factory before shipping to LNF, and a complete report sent together with the magnets. Some of the measurements have been repeated in Frascati to have an independent check, and the longitudinal behaviour of the field, not measured by ASTER, has also been carried out.

The integrated field and the harmonic analysis of high order terms in the quadrupole field have been measured with the Danfysik rotating coil system[1], for both quadrupoles, from now on indicated by #1 and #2. The integrated gradients measured at ASTER and Frascati are given in Tab. 2. It can be seen that the discrepancy between the two measurements is larger than the specified tolerance.

Table 2 - Comparison of ASTER and LNF integrated gradient measurements

	ASTER	LNF
Integrated gradient quad#1 (T)	1.1846	1.2044
Integrated gradient quad#2 (T)	1.1857	1.2048

Table 3 shows the contribution of higher order harmonics (sextupole =2) in the quadrupole field, expressed as the integrated harmonic field divided by the integrated quadrupole field at a distance of 30 mm from the quadrupole axis. Here the agreement between the two measurements is much better.

Table 3 - Higher harmonic contributions to the quadrupole field
Integrated harmonic / Integrated quadrupole @ 30 mm from quadrupole axis

Harmonic	ASTER #1 (%)	LNF #1 (%)	ASTER #2 (%)	LNF #2 (%)
2	.0121	.0111	.0073	.0082
3	.0141	.0140	.0118	.0111
4	.0115	.0116	.0172	.0180
5	.0063	.0067	.0097	.0100
6	.0073	.0073	.0019	.0023
7	.0078	.0076	.0057	.0054
8	.0022	.0016	.0105	.0104
9	.0067	.0065	.0055	.0056
10	.0007	.0006	.0018	.0018

In order to check the specified tolerance on the field quality within the good field region, we have taken the vector sum of all the harmonic contibutions up to the 36-pole with the measured phase. Figure 4 shows the radial and azimuthal components of the field, together with their vector sum, in the case of quadrupole #1, while Fig. 5 is the corresponding one for quadrupole #2. Both magnets meet the specified tolerance.

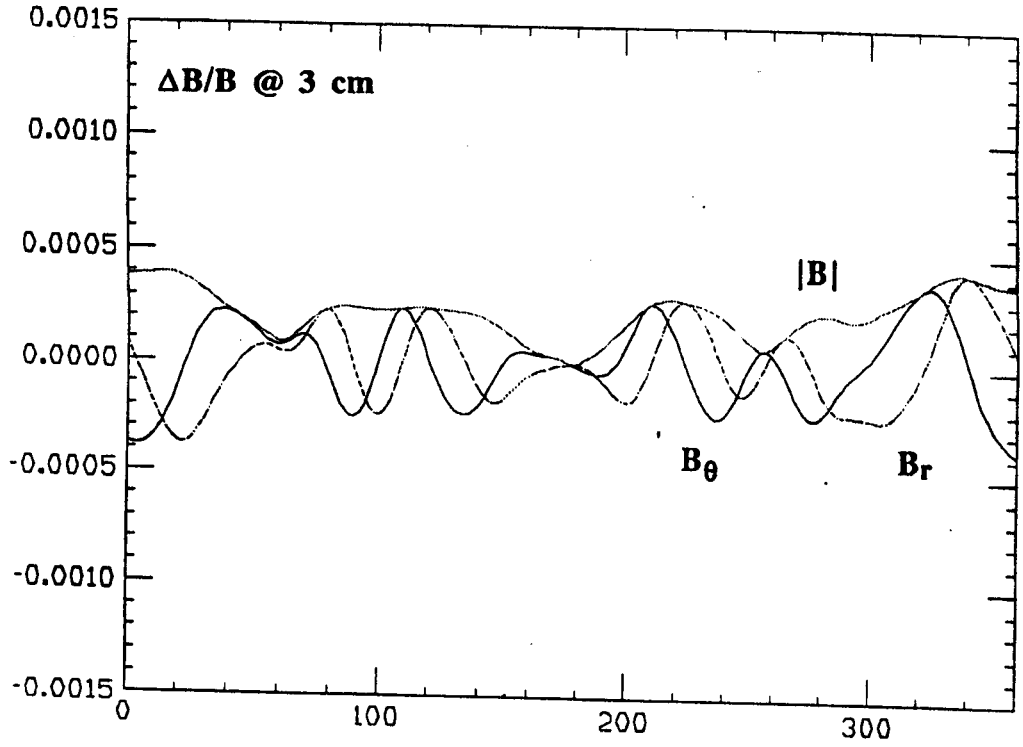

Figure 4 - Vector sum of high order field components in quadrupole #1

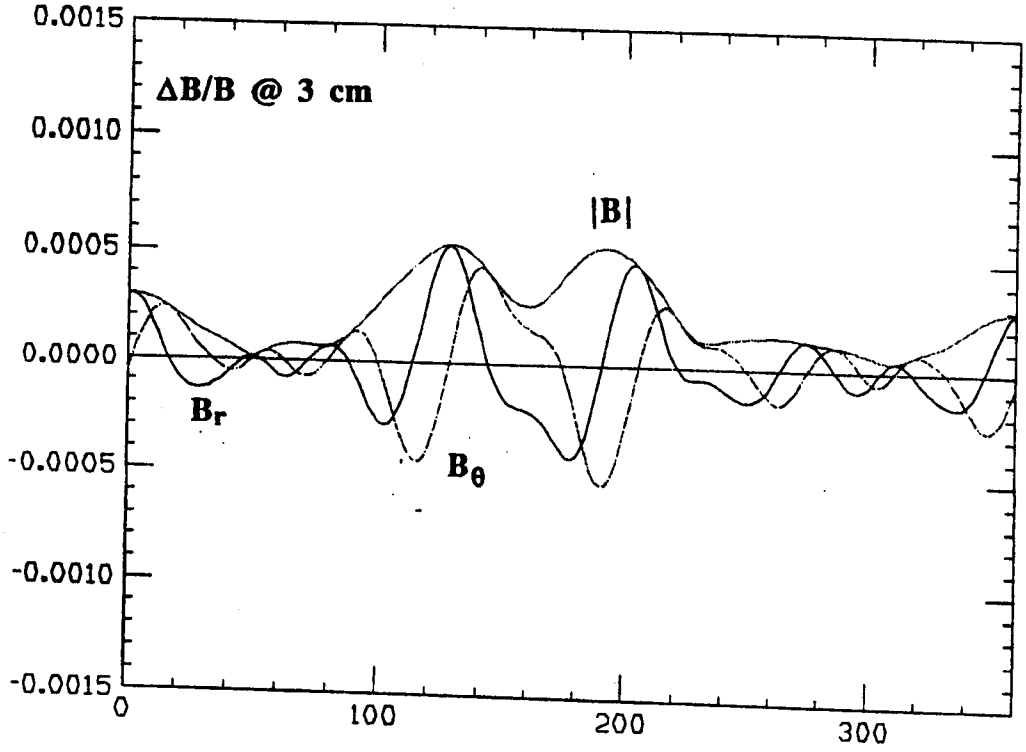

Figure 5 - Vector sum of high order field components in quadrupole #2

An independent measurement of the integrated gradient has been performed with the MicroControle coordinatometer[1] equipped with a GROUP3-MPT-141 Hall probe on quadrupole #1. The vertical component of the field has been measured by moving the probe along straight lines in the horizontal symmetry plane and parallel to the quadrupole axis, at several horizontal distances from it.

Table 5 summarizes the results of the measurement. The columns in the table present the difference between the measurements performed at a given distance r and at r=0, to compensate for the slight disalignment (<0.1 mm) of the coordinatometer.

The same results are presented graphically in Figs. 6 and 7: from both the table and the figures it is possible to see that there is a slight longitudinal asymmetry in the field.

Table 4 shows the integrated field, the magnetic length (defined as the integrated field divided by the maximum field), the integrated gradient (defined as the integrated field divided by the distance from the quadrupole axis) and the longitudinal center of mass position, as a function of the distance from the quadrupole axis.

Table 4 - Integrated field, magnetic length, integrated gradient and center of mass position as a function of radial distance from quadrupole axis.

r (mm)	$\int$ Bds (T.m)	$\int$ Bds / B_{max} (m)	$\int$ Bds / r (T)	r_{av} (mm)
-30	0.036218	0.20155	1.2073	+3.21
-20	0.024149	0.20176	1.2074	+3.21
-10	0.012079	0.20189	1.2079	+3.21
+10	-0.012082	0.20207	1.2082	+3.23
+20	-0.024162	0.20202	1.2081	+3.24
+30	-0.036242	0.20197	1.2081	+3.25

The value of the integrated gradient is in agreement, within the experimental errors, with the measurement performed at LNF with the Danfysik rotating coil system.

Of particular interest for the beam dynamics in the low-β region are the natural high order terms in the fringing field of the quadrupole. We have therefore fitted each row in Tab. 5 with a fifth order polynomial. The behaviour of the 6 coefficients (b0 through b5) is given in Figs. 8÷13 as a function of the longitudinal position.

Table 5 - Vertical component of magnetic field (T) on the horizontal symmetry plane of ASTER quadrupole #1

s(m)	r=-.03	r=-.02	r=-.01	r=0	r=+.01	r=+.02	r=+.028	=+.03
-0.25000	0.00009	0.00006	0.00003	0.00000	-0.00003	-0.00007	-0.00008	0.00008
-0.24000	0.00012	0.00008	0.00005	0.00000	-0.00004	-0.00008	-0.00010	-0.00011
-0.23000	0.00017	0.00011	0.00006	0.00000	-0.00006	-0.00011	-0.00016	-0.00016
-0.22000	0.00023	0.00017	0.00009	0.00000	-0.00009	-0.00017	-0.00023	-0.00023
-0.21000	0.00034	0.00025	0.00014	0.00000	-0.00012	-0.00024	-0.00032	-0.00033
-0.20000	0.00050	0.00036	0.00019	0.00000	-0.00020	-0.00037	-0.00049	-0.00052
-0.19000	0.00078	0.00057	0.00031	0.00000	-0.00030	-0.00057	-0.00074	-0.00078
-0.18000	0.00122	0.00090	0.00048	0.00000	-0.00049	-0.00091	-0.00117	-0.00123
-0.17000	0.00195	0.00146	0.00079	0.00000	-0.00080	-0.00148	-0.00189	-0.00198
-0.16000	0.00324	0.00246	0.00133	0.00000	-0.00133	-0.00246	-0.00314	-0.00326
-0.15000	0.00549	0.00420	0.00228	0.00000	-0.00229	-0.00423	-0.00534	-0.00554
-0.14000	0.00951	0.00730	0.00395	0.00000	-0.00398	-0.00735	-0.00927	-0.00962
-0.13000	0.01676	0.01274	0.00684	0.00000	-0.00688	-0.01283	-0.01631	-0.01695
-0.12000	0.02956	0.02190	0.01156	0.00000	-0.01158	-0.02200	-0.02855	-0.02984
-0.11000	0.05069	0.03593	0.01851	0.00000	-0.01854	-0.03607	-0.04837	-0.05108
-0.10000	0.08063	0.05443	0.02736	0.00000	-0.02740	-0.05455	-0.07582	-0.08106
-0.09000	0.11329	0.07417	0.03676	0.00000	-0.03677	-0.07426	-0.10553	-0.11367
-0.08000	0.13980	0.09100	0.04492	0.00000	-0.04492	-0.09105	-0.12993	-0.14011
-0.07000	0.15724	0.10291	0.05092	0.00000	-0.05090	-0.10294	-0.14617	-0.15732
-0.06000	0.16756	0.11038	0.05480	0.00000	-0.05478	-0.11033	-0.15574	-0.16730
-0.05000	0.17336	0.11475	0.05712	0.00000	-0.05710	-0.11460	-0.16110	-0.17282
-0.04000	0.17648	0.11718	0.05843	0.00000	-0.05843	-0.11702	-0.16412	-0.17594
-0.03000	0.17809	0.11848	0.05916	0.00000	-0.05915	-0.11836	-0.16583	-0.17772
-0.02000	0.17893	0.11918	0.05957	0.00000	-0.05952	-0.11909	-0.16676	-0.17870
-0.01000	0.17941	0.11954	0.05975	0.00000	-0.05974	-0.11948	-0.16726	-0.17923
0.00000	0.17970	0.11969	0.05983	0.00000	-0.05979	-0.11960	-0.16742	-0.17944
0.01000	0.17966	0.11962	0.05977	0.00000	-0.05975	-0.11950	-0.16733	-0.17933
0.02000	0.17918	0.11926	0.05960	0.00000	-0.05957	-0.11916	-0.16689	-0.17887
0.03000	0.17815	0.11855	0.05924	0.00000	-0.05923	-0.11849	-0.16596	-0.17787
0.04000	0.17646	0.11740	0.05865	0.00000	-0.05862	-0.11737	-0.16442	-0.17623
0.05000	0.17396	0.11559	0.05767	0.00000	-0.05767	-0.11560	-0.16214	-0.17385
0.06000	0.17000	0.11257	0.05605	0.00000	-0.05607	-0.11266	-0.15855	-0.17014
0.07000	0.16319	0.10742	0.05332	0.00000	-0.05336	-0.10762	-0.15228	-0.16367
0.08000	0.15122	0.09881	0.04886	0.00000	-0.04891	-0.09906	-0.14105	-0.15193
0.09000	0.13123	0.08542	0.04220	0.00000	-0.04226	-0.08574	-0.12249	-0.13212
0.10000	0.10238	0.06747	0.03355	0.00000	-0.03363	-0.06776	-0.09594	-0.10319
0.11000	0.06994	0.04785	0.02423	0.00000	-0.02428	-0.04804	-0.06612	-0.07040
0.12000	0.04279	0.03072	0.01593	0.00000	-0.01597	-0.03082	-0.04086	-0.04297
0.13000	0.02469	0.01841	0.00976	0.00000	-0.00978	-0.01844	-0.02373	-0.02472
0.14000	0.01399	0.01064	0.00572	0.00000	-0.00574	-0.01066	-0.01349	-0.01400
0.15000	0.00797	0.00610	0.00330	0.00000	-0.00331	-0.00611	-0.00769	-0.00797
0.16000	0.00462	0.00352	0.00190	0.00000	-0.00192	-0.00354	-0.00446	-0.00463
0.17000	0.00274	0.00207	0.00112	0.00000	-0.00112	-0.00208	-0.00265	-0.00275
0.18000	0.00167	0.00125	0.00067	0.00000	-0.00068	-0.00126	-0.00161	-0.00168
0.19000	0.00104	0.00077	0.00041	0.00000	-0.00042	-0.00078	-0.00101	-0.00105
0.20000	0.00066	0.00049	0.00026	0.00000	-0.00027	-0.00050	-0.00065	-0.00068
0.21000	0.00044	0.00032	0.00017	0.00000	-0.00017	-0.00032	-0.00042	-0.00044
0.22000	0.00030	0.00021	0.00012	0.00000	-0.00011	-0.00022	-0.00029	-0.00031
0.23000	0.00020	0.00015	0.00007	0.00000	-0.00008	-0.00015	-0.00020	-0.00021
0.24000	0.00014	0.00010	0.00005	0.00000	-0.00006	-0.00011	-0.00014	-0.00015
0.25000	0.00011	0.00008	0.00004	0.00000	-0.00003	-0.00007	-0.00009	-0.00010

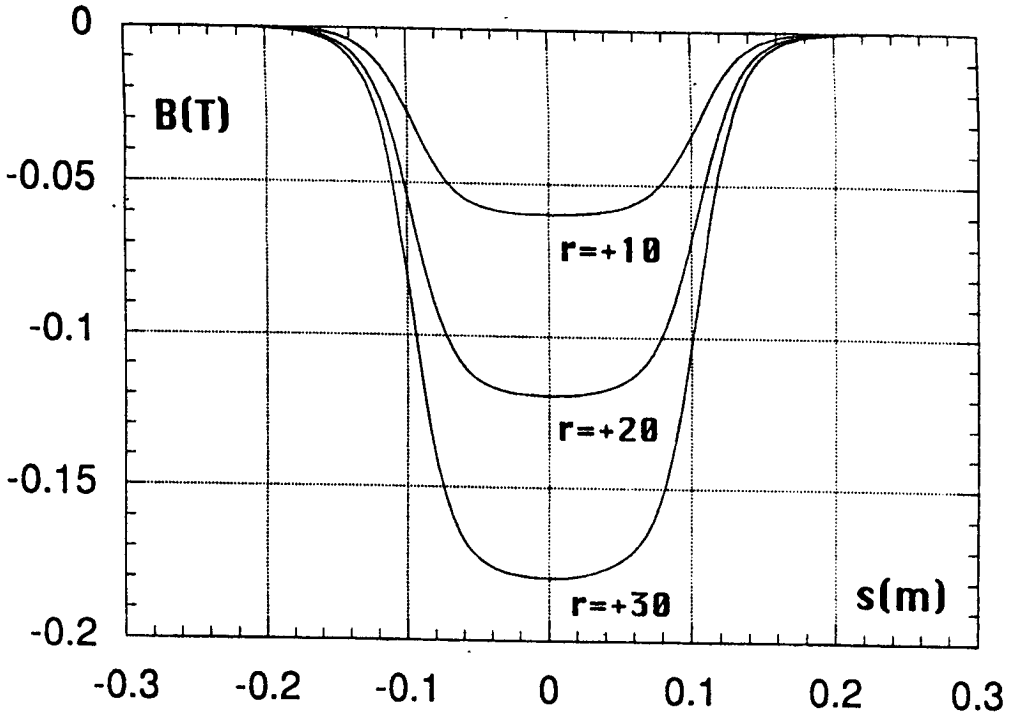

Figure 6 - Longitudinal behaviour of vertical field component at positive distances from quadrupole #1 axis. The longitudinal axis is positive in the direction of the taper (see Fig.1) and towards the interaction point

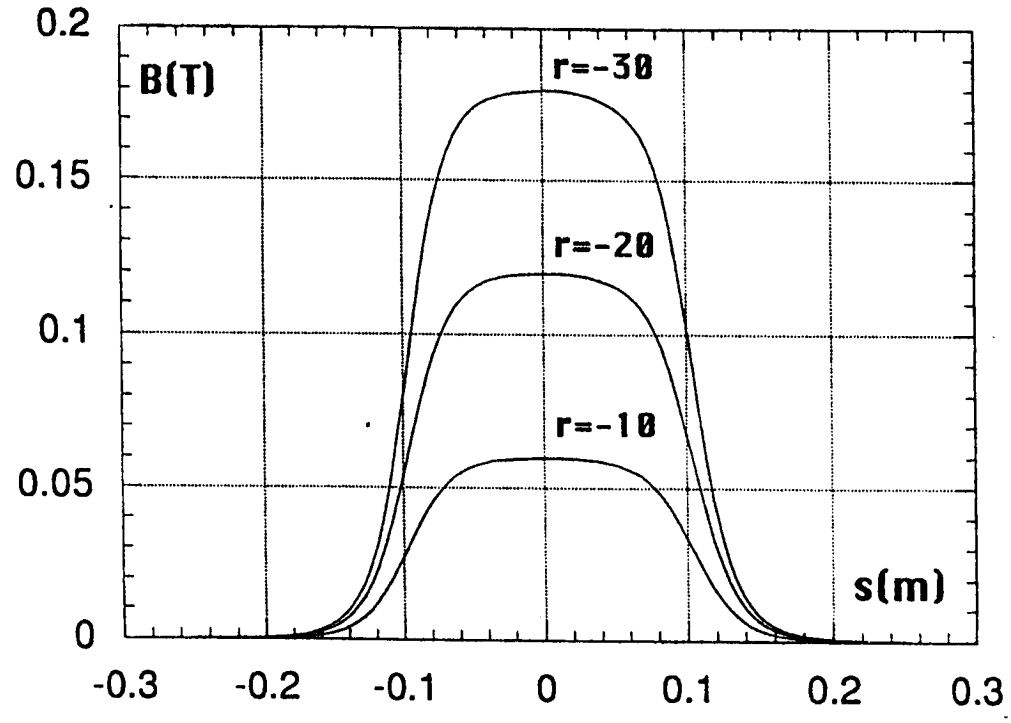

Figure 7 - Longitudinal behaviour of vertical field componentat negative distances from quadrupole #1 axis. The longitudinal axis is positive in the direction of the taper (see Fig.1) and towards the interaction point

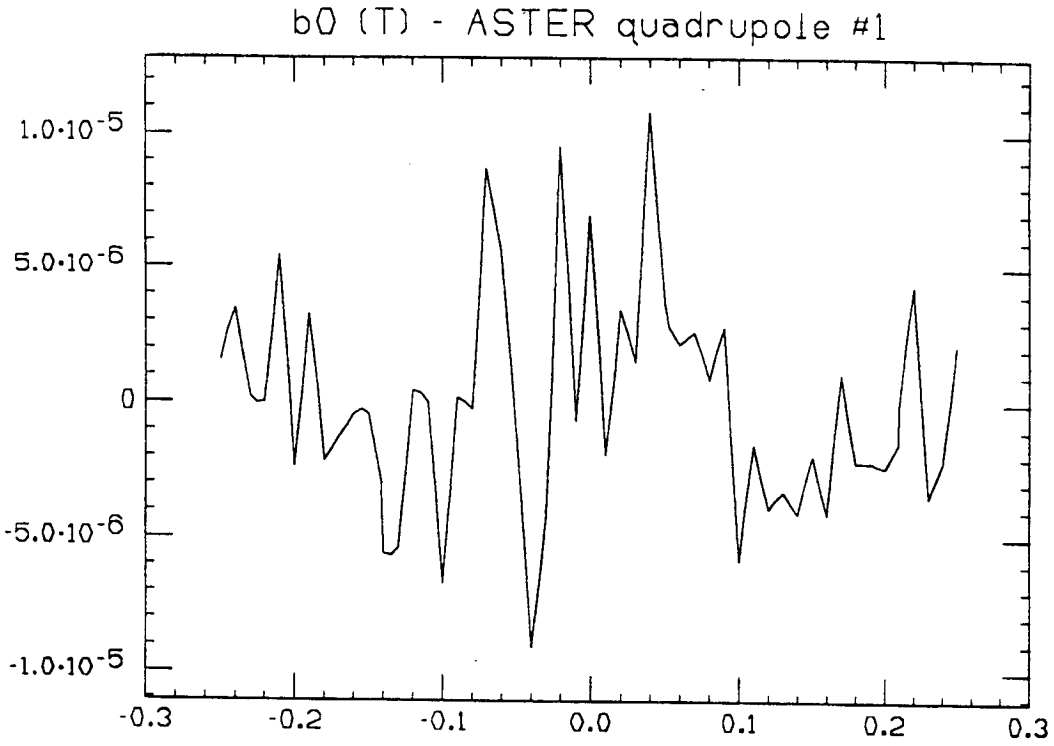

Figure 8 - Longitudinal behaviour of first coefficient of polynomial fit to the transverse dependence of vertical field component

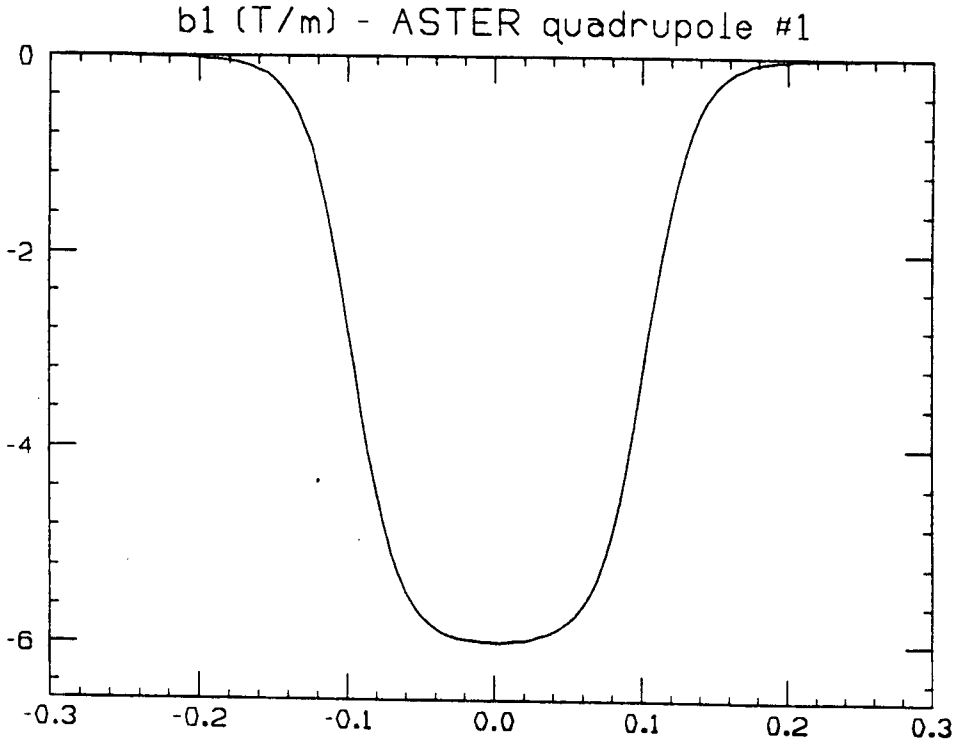

Figure 9 - Longitudinal behaviour of second coefficient of polynomial fit to the transverse dependence of vertical field component

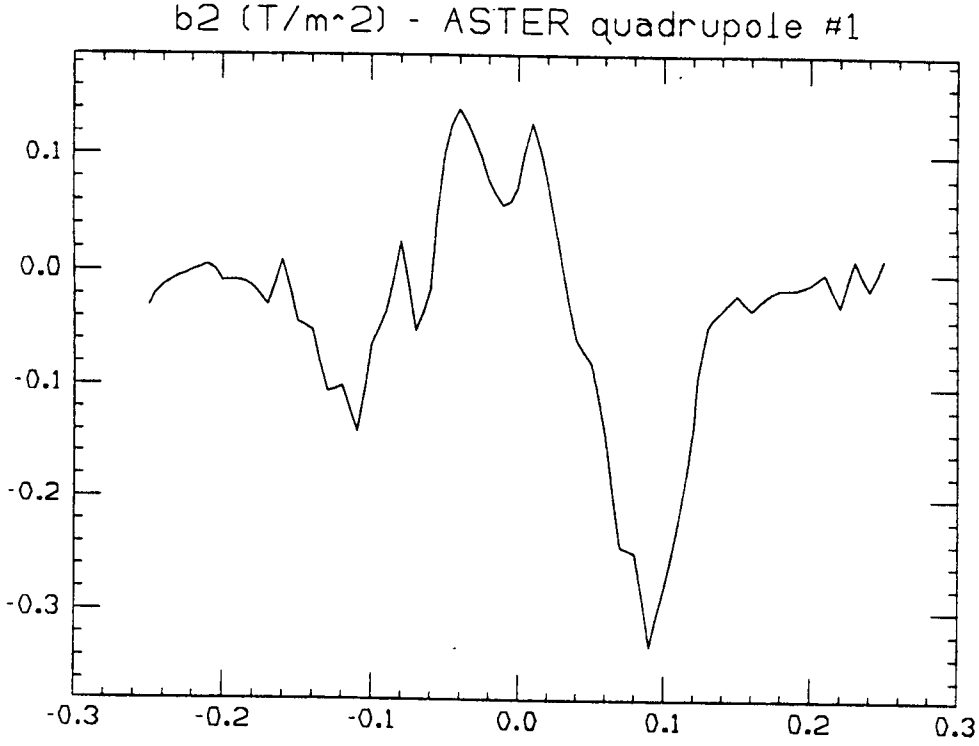

Figure 10 - Longitudinal behaviour of third coefficient of polynomial fit to the transverse dependence of vertical field component

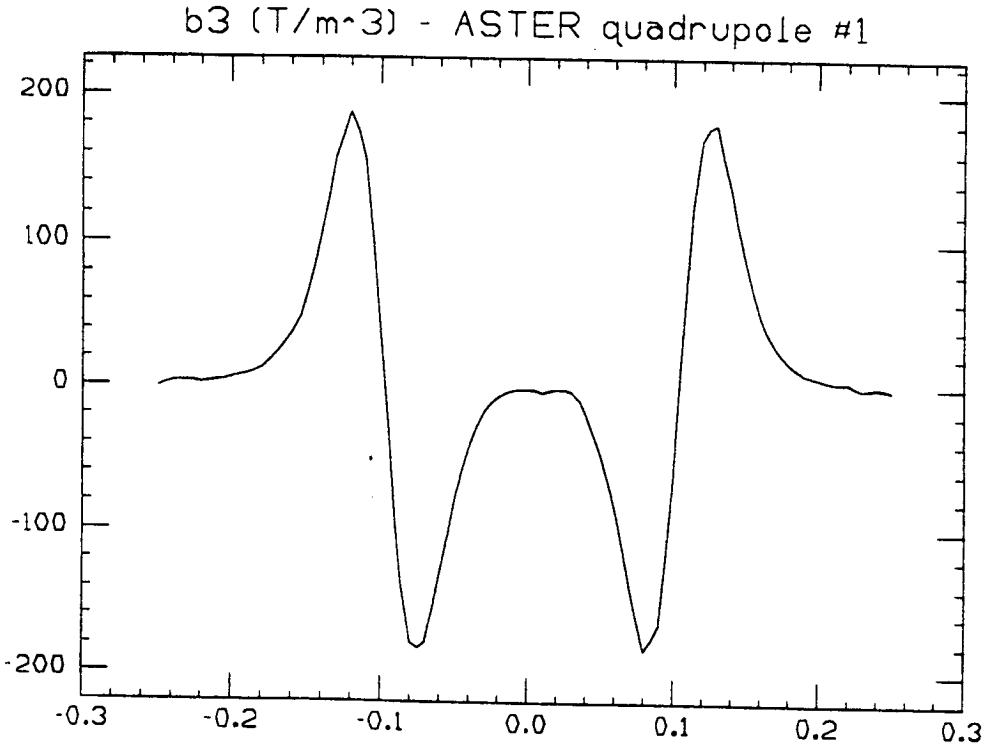

Figure 11 - Longitudinal behaviour of fourth coefficient of polynomial fit to the transverse dependence of vertical field component

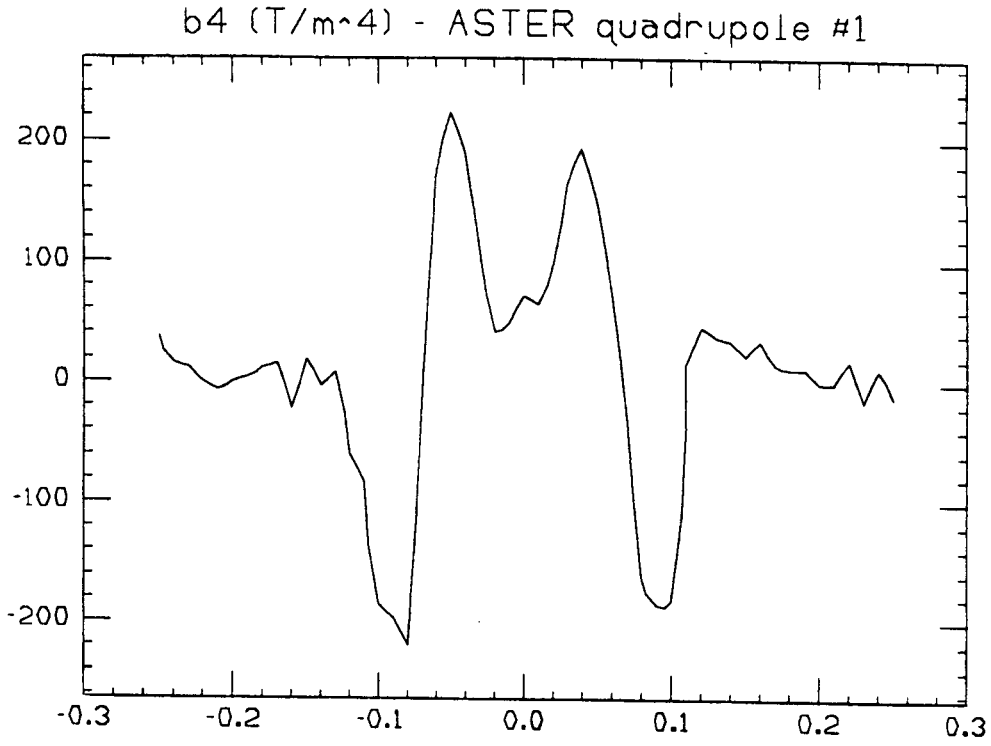

Figure 12 - Longitudinal behaviour of fifth coefficient of polynomial fit to the transverse dependence of vertical field component

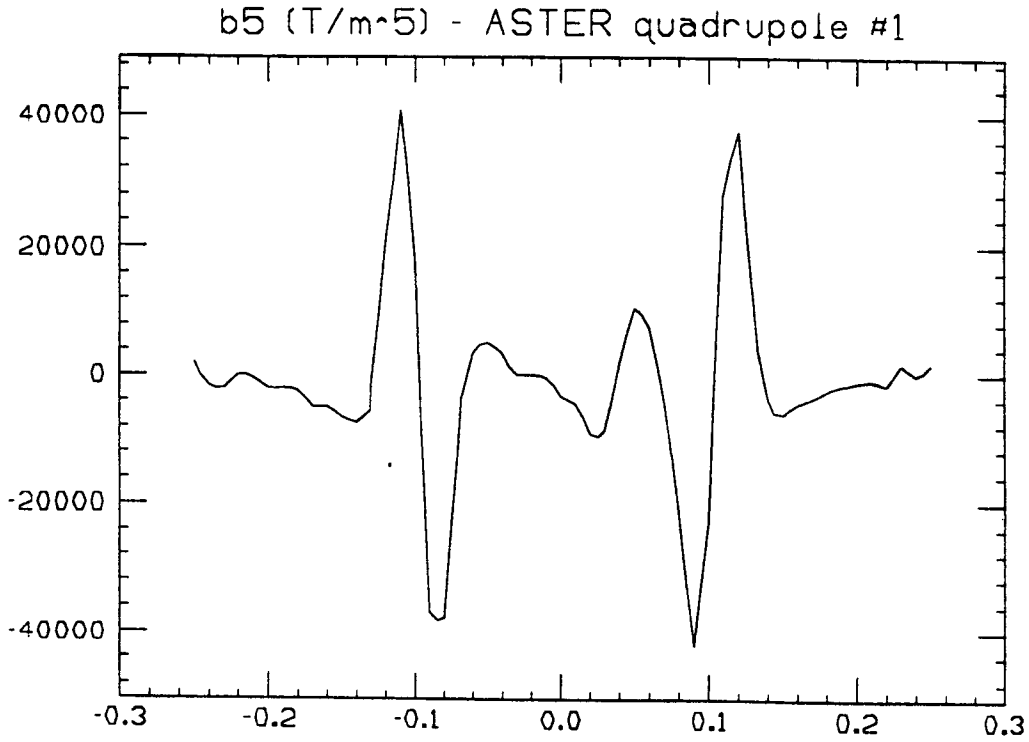

Figure 13 - Longitudinal behaviour of sixth coefficient of polynomial fit to the transverse dependence of vertical field component

3 - MAGNETIC MEASUREMENTS AT CERN

Due to the 1.6% difference in the value of the integrated gradient between ASTER and LNF, we have asked the CERN magnetic measurements group to perform an independent check. Quadrupole #2 has been sent to CERN and the integrated gradient measured with two systems, the first (CERN1) consisting of a rotating coil of the same type as the LNF one, the second (CERN2) of two long and narrow coils separated by a short and narrow one in the center of the magnet to measure both the integrated field at any distance from the quadrupole axis and the magnetic length.

The results are shown in Tab. 6, with the fractional difference taken with respect to the ASTER measurement: the CERN values are higher than both LNF and ASTER ones, but more similar to the results found in Frascati.

Table 6 - Comparison of ASTER. LNF and CERN integrated field measurements on Quadrupole #2

	$\int G\, ds$ (T)	$\Delta(GL)/GL_{Aster}$ (%)
ASTER	1.186	0.0
LNF Rotating Coil	1.205	1.6
LNF Hall Probe	1.208	1.8
CERN1	1.217	2.6
CERN2	1.211	2.1

4 - CHECK LIST

Due to lack of time, the measurements with the Hall probe have not been carried out on quadrupole #2. We plan to do it as soon as possible, since permanent magnets may (at least in principle) change their properties due to demagnetisation phenomena. It is therefore important to keep a complete and up-to-date record of all the measurable characteristics of all the permanent magnet devices installed on the accelerator.

We need also to measure the postion of the magnetic center of both quadrupoles with respect to the alignment system of their supports. This will be done when the final support system of the KLOE Interaction Region will be available.

ACKNOWLEDGMENTS

We are particularly grateful to D. Cornuet and G. Patron of the AT Group in CERN for performing the magnetic measurements on the DAΦNE permanent magnet quadrupole.

REFERENCES

[1] F. Iungo, M. Modena, Q. Qiao, C. Sanelli: "DAΦNE Magnetic measurements systems", DAΦNE Technical Note MM-1 (4/11/1993).